Original Research

Visible Light-Driven Photocatalytic Degradation of 1,2,4-trichlorobenzene with Synthesized Co$_3$O$_4$ Photocatalyst

Chuang Wang[1, 2], Bozhi Ren[1, 2, 3]*, Andrew S Hursthouse[1, 4], Baolin Hou[1, 2], Yazhou Peng[1,2]

[1]Hunan Provincial Key Laboratory of Shale Gas Resource Exploitation, Xiangtan, P.R. China
[2]School of Civil Engineering, Hunan University of Science and Technology, Xiangtan, P.R. China
[3]Key Laboratory of Theoretical Organic Chemistry and Functional Molecule, Ministry of Education, Xiangtan, P.R. China
[4]School of Science and Sport, University of the West of Scotland, Paisley, United Kingdom

Abstract

A cubic crystal form Co$_3$O$_4$ was synthesized using the sol-gel method and applied as catalyst in the visible light-driven photocatalytic degradation of 1,2,4-trichlorobenzene (1,2,,4-TCB). 1,2,4-TCB removal efficiency initially increased and was followed by a gentle decrease as the Co$_3$O$_4$ dosage increased, with the optimal dosage of 2.0 g/L. The degradation rate changed positively with light intensity and reaction temperature. However, pH exerted only a slight effect on 1,2,4-TCB degradation. Strong acidic and basic conditions were conducive to the photocatalytic degradation of 1,2,4-TCB. The optimal parameters for the photocatalytic degradation of 1,2,4-TCB were found at a Co$_3$O$_4$ dosage of 2.0 g/L, 350 W of illumination intensity, initial 1,2,4-TCB concentration of 7.5 mg/L at 30ºC, with 1,2,4-TCB removal efficiency of 90.13% after 6.0 hours photocatalytic degradation. The Co$_3$O$_4$ synthesized in the study with high-purity and stable properties guaranteed its high catalytic activity and stability. The possible mechanisms of visible light-driven photocatalytic degradation of 1,2,4-TCB with synthesized Co$_3$O$_4$ photocatalyst were also proposed.

Keywords: visible light-driven photocatalyst, Co$_3$O$_4$, photocatalytic degradation, 1,2,4-TCB

Introduction

As persistent organic pollutants (POPs), chlorobenzenes (CBs) have been widely used in industrial and agricultural production of pharmaceuticals, petrochemicals, and pesticides and in the process have become common pollutants [1] found in air, soils [2-3], sludge [4], lake and coastal sediments [5], ground-water, and river entrances [6-7]. Trichlorobenzene is a common type of CB, with 3 isomers, including 1,2,4-TCB, which is the most widely used for industrial purposes and once was made widely available in the electrochemical industry as a substitute of

*e-mail: renbz2016@163.com

polychlorinated biphenyls [8-9]. The widespread use of 1,2,4-TCB makes it one of the highest concentrations of chlorinated organic pollutants in the environment. 1,2,4-TCB has been found in soils [10-11], groundwater, wastewater [12], activated sludge, and vegetables [1, 13]. CBs are of poor biodegradability, high toxicity, and stable chemical structure, and may accumulate in organisms through the food chain and result in mutagenesis, carcinogenesis, and teratogenesis – greatly endangering human health and ecological environment.

The usual methods of dealing with CBs are heat treatment [14], biodegradation [8, 15], advanced oxidation process (AOPs), and carbon adsorption. These methods have a number of limitations. Traditionally, CBs are destroyed through high-temperature incineration, which requires high reaction temperatures and has the potential to generate more toxic dioxin-like chemicals. Although biodegradation and charcoal adsorption are effective and can react at room temperature and do not generate toxic dioxin-like chemicals, the application of these approaches is expensive, time-consuming, and difficult to apply consistently in engineering practice. The AOPs can break non-biodegradable organic matter into molecules of low- to non-toxicity, and may deal with CBs effectively. Currently, advanced oxidation technologies need to be further studied to push through bottlenecks of engineering applications and promote use more widely. Photocatalysis in AOPs and combined processes are becoming popular in water treatment. Highly efficient and environmentally benign photocatalysts play a critical role in the whole process. As a traditional photocatalyst, TiO_2 has been widely used in the fields of energy and the environment [16-18], but yields a low photocatalytic effect due to its reaction under UV light and recombination of photo-induced electron holes [19]. Therefore, extending the photocatalytic activity of photocatalysts into the visible range becomes an important topic of photocatalysis-related research.

Other metal oxides with low cost and high catalytic activity, good thermal stability, large specific surface area, and a facile preparation method are essential drivers for the successful application of a catalyst [20-22]. As a transition metal oxide, Co_3O_4 is formally a spinel-type structure, with the lattice being composed of regular tetrahedrons (oxygen ions covering Co^{2+}) and regular octahedrons (oxygen ions covering Co^{3+}) [23]. With empty electron orbitals, Co_3O_4 may accept and transfer electrons, forming stable complexes and accelerating reactions, so Co_3O_4 has risen in significance in terms of catalyst applications [24].

In this study, Co_3O_4 was synthesized using the sol-gel method and served as a photocatalyst in visible light-driven photocatalytic degradation of 1,2,4-TCB. The degradation performance was evaluated under a range of experimental variables and the photocatalytic mechanism was discussed preliminarily.

Materials and Methods

Chemicals

1,2,4-TCB was purchased from Dongguan Qiaosun Fine Chemicals Co., Ltd. Cobalt-nitrate hexahydrates were purchased from Xilong Scientific Co., Ltd. Hydrogen peroxides (30%), ethyl acetate, and n-hexanes were purchased from Guangdong Guanghua Sci-Tech Co., Ltd. All chemicals were analytical grade reagents and were used directly without further purification. The reaction medium was deionized water.

Preparation of Co_3O_4 Photocatalyst

The Co_3O_4 used in our research was synthesized according to the following process: 11.06 g cobalt nitrate hexahydrate was dissolved with 80 ml absolute ethyl alcohol in a 250 ml beaker and the solution was stirred slowly for 2.0 hours at 50ºC. Then 80 ml ethyl acetate was added slowly with stirring until a uniform mixture was obtained. The mixture was heated with a heating jacket to boiling and cooled. Then the mixture was transferred to a 250 ml conical flask for 16 hours of reflux and condensation at 50ºC to reduce solution volume to 1/3 of the initial volume. The refluxed mixture was evaporated for 12 hours at 80ºC, then calcined at 450ºC for 2.0 hours. Finally, the calcined sample was cooled and stored in a desiccator prior to use.

Experimental Procedures

Visible-light-driven photocatalytic degradation of 1,2,4-TCB was conducted in a 300 mL cylindrical glass reactor. A spherical xenon lamp with adjustable power was used as a simulated visible light source (maximum power of 350 W). A UV cut-off filter allowed for the passage of light within the wavelength range between 400 nm to 800 nm, in which the visible light transmittance exceeded 97%, eliminating the effect of UV light on photocatalysis. The glass beaker was covered with plastic wrap to prevent water evaporation and was wrapped with silver papers to eliminate the disturbance from external visible light around the reaction vessel.

Portions of Co_3O_4 were added into the 300 mL beaker, followed by 250 mL of water containing appropriate concentrations of 1,2,4-TCB. The beaker was covered with the UV cut-off filter and stirred with a magnetic stirrer under illumination with the xenon lamp. Samples were withdrawn at pre-selected time intervals (0.5 h) filtered with 0.45 μm filter paper and stored at 4ºC for further analysis.

Analytical Methods

1,2,4-TCB concentration was measured by GC (GC2010-plus) equipped with EDC (RTX-1). Samples were pretreated with filtration and extraction before
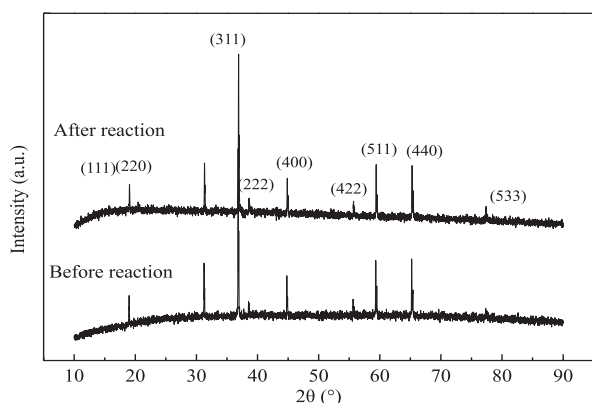
Fig. 1. XRD pattern of Co_3O_4 before and after catalytic reaction.

the injection to GC. Chromatographic conditions were: detector temperature 260ºC; injection port temperature 240ºC; procedure for rise of chromatographic column temperature – keep at 90ºC for 1.0 min, increase to 140ºC at 10ºC/min, and then increase to 200ºC at 20ºC/min and maintain for 1.0 min; carrier gas was nitrogen; split ratio 5:1; and column flow 2.0 mL/min. The crystal structures of Co_3O_4 were examined with an x-ray diffractometer (XRD, Bruker AXS GmbH). Surface morphology was characterized on a field-emission scanning electron microscope (SEM, JSM-6380LV).

All the experiments were repeated in triplicate, and the results given were the average for three replicates with a relative standard deviation of less than 5%.

Results and Discussion

Catalyst Characterization

XRD was used to characterize the crystal structures of the synthesized Co_3O_4 catalyst (Fig. 1). The diffraction peaks at 18.99°, 31.25°, 36.84°, 38.53°, 44.79°, 55.63°, 59.35°, 65.22°, and 77.39° are respectively assigned to the (111), (220), (311), (222), (400), (422), (511), (440), and (533) planes of the cubic-phase Co_3O_4 structure, according to the standard card of Co_3O_4 (JCPDS card NO. 42-1467) [25-26]. The XRD patterns of Co_3O_4 before reaction has sharp peaks, and the main diffraction angles consistent with interfacial diffraction peaks and without unassigned impurity peaks, show that the Co_3O_4 samples were of high purity and fully crystallized cubic crystals. By comparison, between the XRD patterns of Co_3O_4 before and after reaction, no obvious difference is observed, consistent with cubic-phase Co_3O_4 crystal characteristic peaks (JCPDS card No. 42-1467). The results show that the synthesized Co_3O_4 is of high stability, and may be effectively recycled as a good catalyst with potential applications.
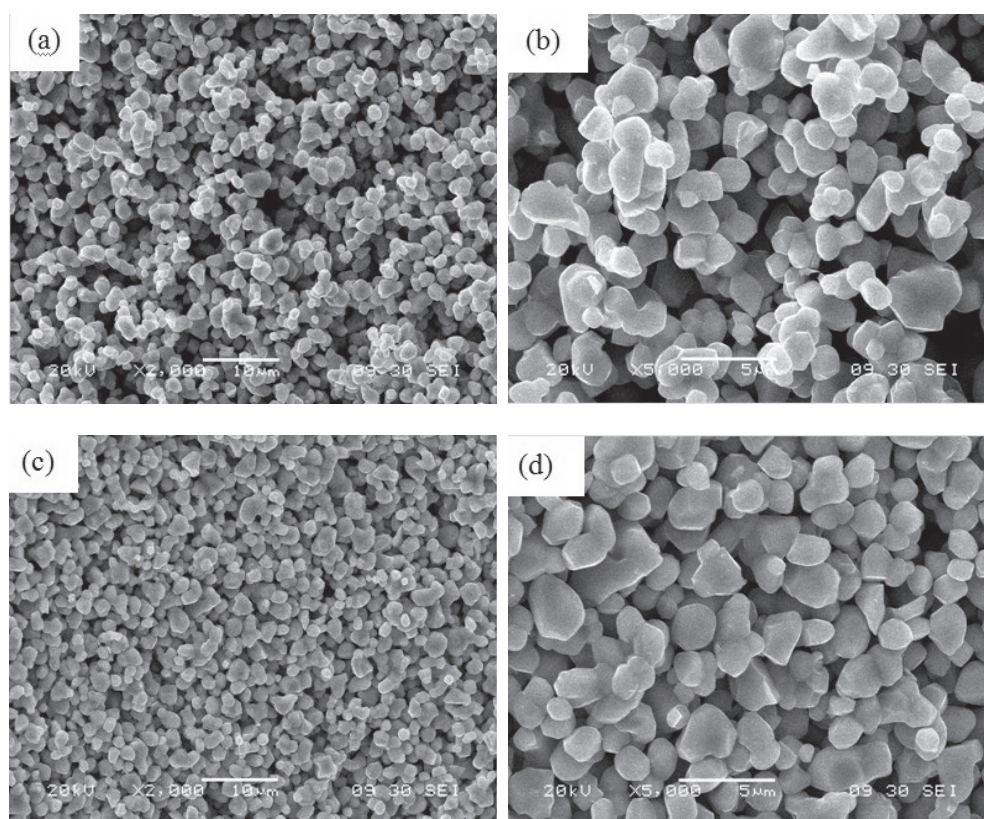

Fig. 2. SEM images of the synthesized Co_3O_4: a) ×2000 before reaction, b) ×5000 before reaction, c) ×2000 after reaction, and d) ×5000 after reaction.
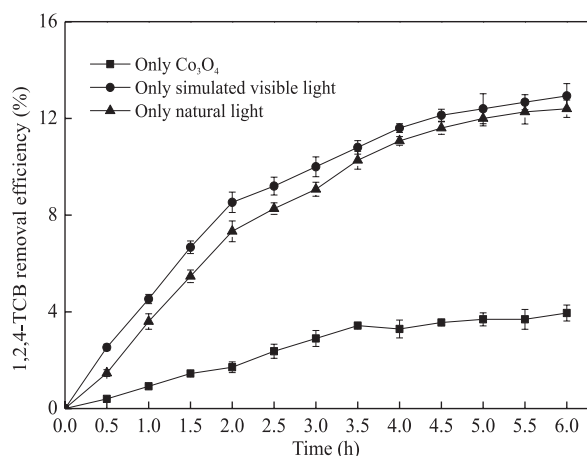
Fig. 3. Blank experiments (experimental conditions: initial 1,2,4-TCB concentration 7.59 mg/L, Co_3O_4 dosage 2.0 g/L, temperature 25ºC, illumination intensity 350 W).

during the experiments. The results are illustrated in Fig. 3. In addition, the blank experiment was also used to verify the feasibility of the use of a spherical xenon lamp as a simulated visible light source in subsequent experiments. A trial with a natural light source was conducted at 10-16:00 at 23-28ºC on a sunny day.

In the absence of light, 1,2,4-TCB removal efficiency was less than 4% after 6.0 hours reaction, indicating that Co_3O_4 has a minimal effect on 1,2,4-TCB removal. Under the action of unassisted photodegradation with simulated visible light or natural light, 1,2,4-TCB removal efficiencies were both less than 13% after 6 hours of illumination, with simulated light showing a slightly higher effect. Within the scope of our survey, a negligible difference in 1,2,4-TCB removal was obtained under simulated visible light and natural light, demonstrating that it is feasible to use the spherical xenon lamp as simulated visible light.

Photocatalytic Degradation Performance of 1,2,4-TCB

Effect of Co_3O_4 Dosage

The dosage of Co_3O_4 has a significant effect on 1,2,4-TCB degradation (Fig. 4). 1,2,4-TCB removal efficiency improves dramatically after the addition of Co_3O_4. The degradation rate of 1,2,4-TCB degradation initially rapidly increased before peaking into a more gentle decline. The optimal dosage was 2.0 g/L, with 1,2,4-TCB removal efficiency of ~86% after 6.0 hours of photocatalysis. When the Co_3O_4 dosage increased to 4.0, 6.0, and 8.0 g/L, 1,2,4-TCB removal efficiency decreased to ~80%, 77%, and 74%, respectively. The explanation is that the number of photo-induced electron-hole pairs are relatively low at the initial Co_3O_4 dosage, resulting in lower 1,2,4-TCB removal efficiency. Increasing the photocatalyst dosage resulted in an increase in the probability of catalyst exposure to 1,2,4-TCB, therefore

The surface morphology

The surface morphology of the synthesized Co_3O_4 was analyzed via SEM (Fig. 2). The cubic Co_3O_4 crystals with the average grain diameter of 2.0 μm are observed and visually are distributed in a uniform manner. There are changes in the particle distribution of the Co_3O_4 before and after reaction. After reaction, the particles show fewer large pore spaces and no changes in the visual size and shape with no new structural substances formed. The stability of Co_3O_4 displayed by SEM was consistent with the analysis of XRD.

Blank Experiment for 1,2,4-TCB Degradation

To exclude the effect of self-degradation and adsorption on the apparent removal of 1,2,4-TCB in the photocatalytic reaction, blank experiments were conducted to investigate the contributions of self-degradation and adsorption on the removal of 1,2,4-TCB
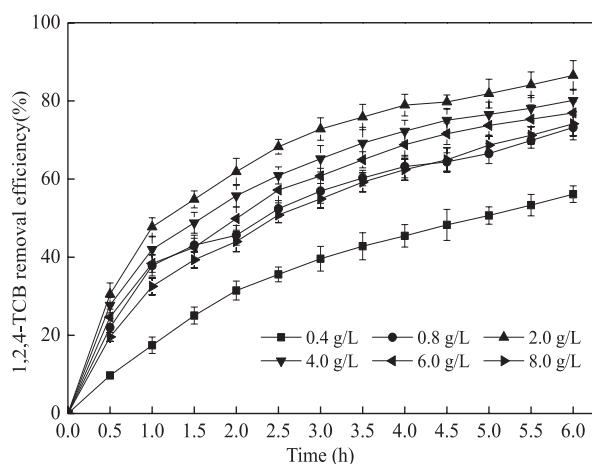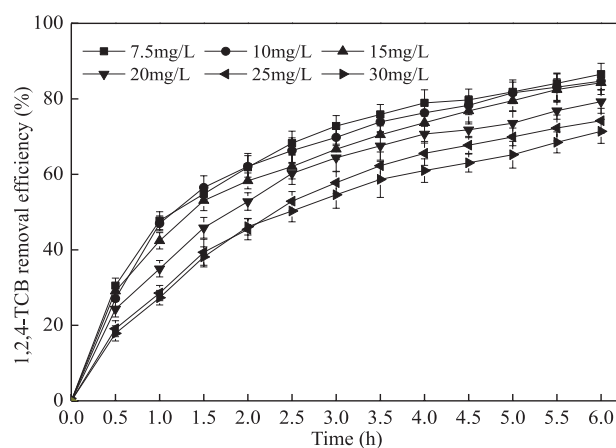

Fig. 4. Effect of Co_3O_4 dosage on the degradation of 1,2,4-TCB (experimental conditions: illumination intensity 350 W, initial concentration 7.5 mg/L, temperature 25ºC).

Fig. 5. Effect of initial concentration on 1,2,4-TCB degradation (experimental conditions: illumination intensity 350 W, Co_3O_4 dosage 2.0 g/L, temperature 25ºC).
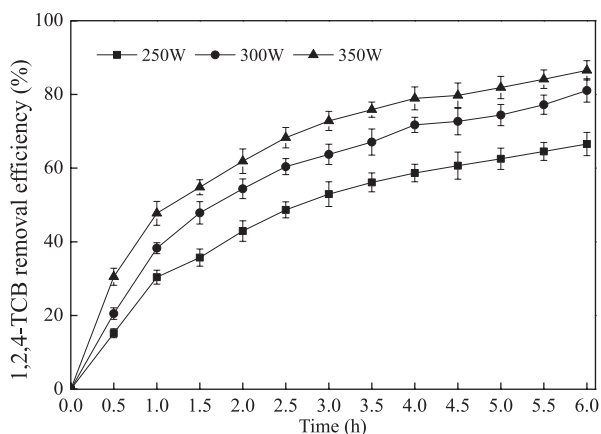
Fig. 6. Effect of illumination intensity on 1,2,4-TCB degradation (experimental conditions: Co_3O_4 dosage 2.0 g/L, initial concentration 7.5 mg/L, temperature 25ºC).

improving photocatalytic efficiency. Beyond the optimal dosage, the presence of an increased amount of photocatalyst obstructed the transmittance of visible light in liquid solution and reduced the generation of electron-hole pairs and a reduction in photocatalytic degradation of 1,2,4-TCB [27-28].

Effect of Initial 1,2,4-TCB Concentration

1,2,4-TCB removal efficiency gradually decreased from 86% to 84% for 6.0 hours of photocatalysis time when the initial concentration increased from 7.5 to 30 mg/L (Fig. 5). The results showed that the synthesized Co_3O_4 produced a good effect in 1,2,4-TCB removal when the initial concentration was less than 15 mg/L, with removal efficiency higher than 84%. When the starting concentration continued to increase,
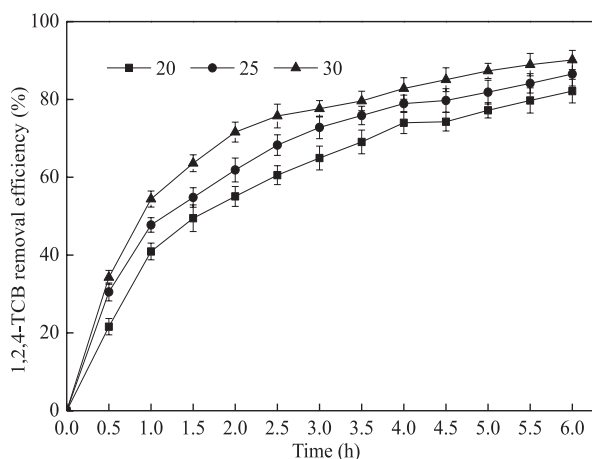
removal efficiency greatly descreased. This may be due to degradation intermediates competing with 1,2,4-TCB for the fixed photo-induced electron-hole pairs and when initial starting concentration is high. Moreover, with a higher contaminant concentration, higher turbidity may have affected the transmission of light and thus reduced the degradation rate.

Effect of Illumination Intensity

Illumination is the power for photocatalysis. The effect of illumination intensity on the visible light-driven photocatalytic degradation of 1,2,4-TCB was conducted and illustrated in Fig. 6.

Illumination intensity had a significant effect on 1,2,4-TCB removal (Fig. 8). The 1,2,4-TCB removal efficiencies were 66%, 81%, and 86%, respectively, when illumination intensities were 250 W, 300 W, and 350 W.

As the energy source for driving the photocatalytic reaction, the reduction of illumination intensity certainly affected photon density and the irradiance in reaction vessels and reduced the probability of photon exposure to activate sites on the Co_3O_4, thus lowering 1,2,4-TCB removal efficiency [29-30].

Effect of Reaction Temperature

The 1,2,4-TCB removal efficiencies were 82%, 87%, and 90%, respectively, when the reaction temperature was maintained at 20°°C, 25ºC, and 30ºC (Fig. 7). The degradation of 1,2,4-TCB was enhanced with the increase of reaction temperature of only a few degrees. With the rise of reaction temperature and acceleration of reaction, the desorption of water by active sites on the Co_3O_4 intensified, increasing the probability of exposure to 1,2,4-TCB and thus enhancing the degradation of 1,2,4-TCB [31-32].
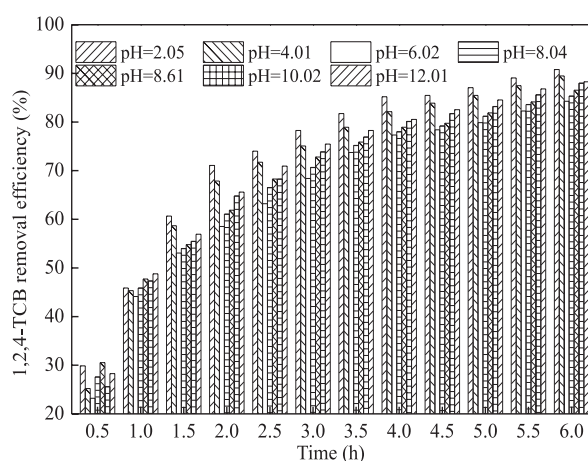

Fig. 7. Effect of reaction temperature on 1,2,4-TCB degradation (experimental conditions: illumination intensity 350 W, Co_3O_4 dosage 2.0 g/L, initial concentration 7.5 mg/L).
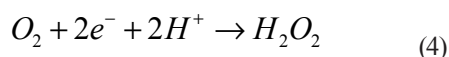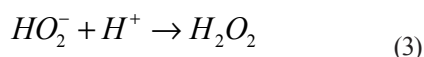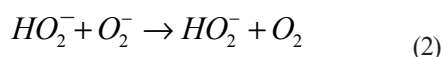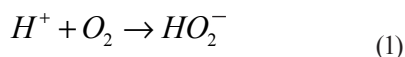

Fig. 8. Effect of pH on 1,2,4-TCB degradation (experimental conditions: illumination intensity 350 W, Co_3O_4 dosage 2.0 g/L, initial concentration 7.5 mg/L, temperature 25ºC).

Effect of pH

The pH of reaction medium affected the state of the compound in solution. The effect of pH on 1,2,4-TCB degradation is shown in Fig. 8.

As the pH was adjusted between 2.0 and 12.0, the removal efficiency for 1,2,4-TCB decreased, reaching a minimum of around pH 6.0 before increasing to levels similar at the start. Stronger acid conditions are conducive to the photocatalytic degradation of 1,2,4-TCB. The pH_{PZC} of the synthesized Co_3O_4 was close to neutral, where the electrostatic force of Co_3O_4 surface was greater than the neutral water, resulting in the clustering of Co_3O_4 particles and a reduction of the specific surface area and active sites. When pH was less than or more than the pH_{PZC}, the Co_3O_4 surface was positively or negatively charged, inducing dispersion of the Co_3O_4 increasing the specific surface area and active sites enhancing the photocatalytic degradation of 1,2,4-TCB. In addition, pH affected the photocatalytic reactions (Eq. (1-4)) and the redox activity of radicals.

$$H^+ + O_2 \rightarrow HO_2^- \tag{1}$$

$$HO_2^- + O_2^- \rightarrow HO_2^- + O_2 \tag{2}$$

$$HO_2^- + H^+ \rightarrow H_2O_2 \tag{3}$$

$$O_2 + 2e^- + 2H^+ \rightarrow H_2O_2 \tag{4}$$

Photocatalytic Mechanism

It is generally accepted that degradation and/or mineralization of organic molecules is ascribed to the free radicals produced in the photocatalytic reactions. H^+, $\cdot OH^-$, and $\cdot O_2^-$, etc. are suspected of being involved in this visible light-driven photocatalytic degradation of 1,2,4-TCB with the synthesized Co_3O_4 photocatalyst [23, 29].

Dechlorination process of 1,2,4-TCB was expected to be stepwise. Dichlorobenzene (DCB, o-DCB, m-DCB, p-DCB), monochlorobenzene (MCB), chlorophenol, and several aliphatic acids were detected during the degradation of 1,2,4-TCB. For 1,2,4-TCB the theoretical bond dissociation energies corresponding to C-Cl(1), C-Cl(2), and C-Cl(4) are 373.71 kJ/mol, 370.98 kJ/mol, and 378.33 kJ/mol, respectively [24]. In the molecule structure of 1,2,4-TCB, the Cl(2) is easier to be dissociated since the bond dissociation energy of C–Cl(2) is the lowest according to density functional theory (DFT) analysis of the 1,2,4-TCB molecule. The dechlorination of Cl(2) of 1,2,4-TCB resulted in the formation of p-DCB. Then another Cl in p-DCB was dissociated, forming MCB. MCB was degraded to be aliphatic acids, Cl⁻, and CO_2 by the radicals such as h^+, $\cdot OH$, and $\cdot O_2^-$. The possible photocatalytic mechanism and the degradation pathway of 1,2,4-TCB in the photocatalytic reactions with the synthesized Co_3O_4 photocatalyst were proposed and are depicted in Fig. 9.
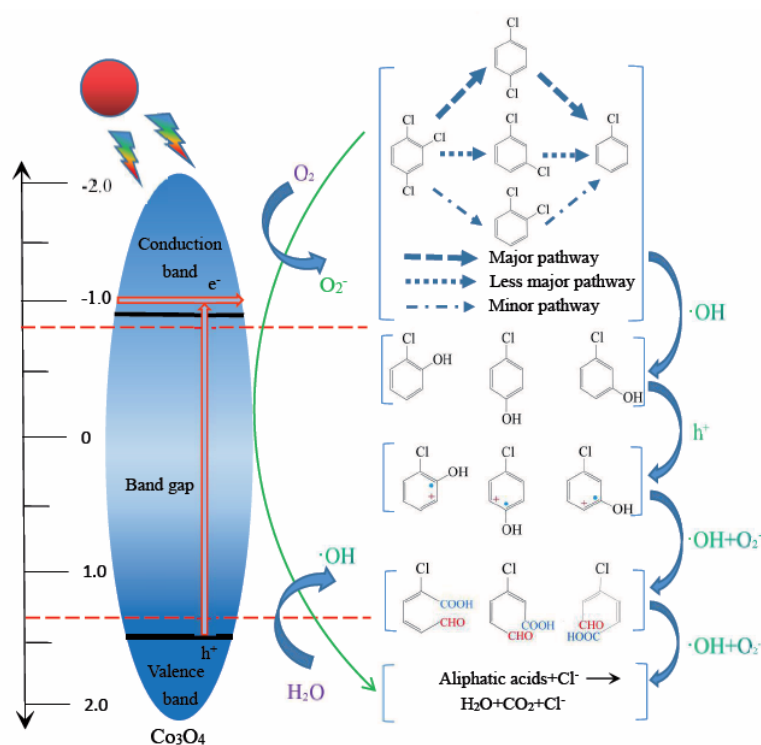

Fig. 9. Possible mechanism of visible light-driven photocatalytic degradation of 1,2,4-TCB with synthesized Co_3O_4 photocatalyst.

Conclusions

Cubic Co_3O_4 was synthesized with high purity and uniform size distribution. The synthesized Co_3O_4 exhibited excellent catalytic activity in the photocatalytic degradation of 1,2,4-TCB under visible light. Co_3O_4 dosage, 1,2,4-TCB initial concentration, illumination intensity, and reaction temperature affected the photocatalytic degradation of 1,2,4-TCB dramatically, while pH exerted a slight effect on 1,2,4-TCB degradation. Strong acidic and basic conditions were conducive to the photocatalytic degradation of 1,2,4-TCB. The optimal parameters for the photocatalytic degradation of 1,2,4-TCB were 2.0 g/L of Co_3O_4 dosage, 350 W of illumination intensity, 7.5 mg/L of initial 1,2,4-TCB concentration at 30ºC, with 1,2,4-TCB removal efficiency of 90.13% after 6.0 hours of photocatalytic degradation. Moreover, the synthesized Co_3O_4 showed high stability in the photocatalytic reaction, which is beneficial to its practical application.

Acknowledgements

References

1. ZHANG J.Y., ZHAO W., PAN J., QIU L.M., ZHU Y.M. Tissue-dependent distribution and accumulation of chlorobenzenes by vegetables in urban area. Environment International, **31** (6), **2005**.

2. DONG W.H., ZHANG P., LIN X.Y., ZHANG Y., TABOURE A. Natural attenuation of 1,2,4-trichlorobenzene in shallow aquifer at the Luhuagang's landfill site, Kaifeng, China. Science of the Total Environment, **505**, **2015**.

3. WANG H., HWANG J., HUANG J., XU Y., YU G., LI W., ZHANG K., LIU K., CAO Z., MA X., WEI Z., WANG Q. Mechanochemical remediation of PCB contaminated soil. Chemosphere, **168**, **2017**.

4. BARBER J.L., SWEETMAN A.J., VAN WIJK D., JONES K.C. Hexachlorobenzene in the global environment: Emissions, levels, distribution, trends and processes. Science of the Total Environment, **349** (1-3), **2005**.

5. HUO S., LI C., XI B., YU Z., YEAGER K.M., WU F. Historical record of polychlorinated biphenyls (PCBs) and special occurrence of PCB 209 in a shallow fresh-water lake from eastern China. Chemosphere, **184**, **2017**.

6. ANIM A.K., DRAGE D.S., GOONETILLEKE A., MUELLER J.F., AYOKO G.A. Distribution of PBDEs, HBCDs and PCBs in the Brisbane River estuary sediment. Marine Pollution Bulletin, **120** (1), **2017**.

7. LU Q., FUTTER M.N., NIZZETTO L., BUSSI G., JÜRGENS M.D., WHITEHEAD P.G. Fate and transport of polychlorinated biphenyls (PCBs) in the River Thames catchment - Insights from a coupled multimedia fate and hydrobiogeochemical transport model. Science of the Total Environment, **572**, **2016**.

8. SCHROLL R., BRAHUSHI F., DORFLER U., KUHN S., FEKETE J., MUNCH J.C. Biomineralisation of 1,2,4-trichlorobenzene in soils by an adapted microbial population. Environmental Pollution, **127** (3), **2004**.

9. TAKEUCHI S., ANEZAKI K., KOJIMA H. Effects of unintentional PCBs in pigments and chemical products on transcriptional activity via aryl hydrocarbon and nuclear hormone receptors. Environmental Pollution, **227**, **2017**.

10. ZOLEZZI M., CATTANEO C., TARAZONA J.V. Probabilistic ecological risk assessment of 1,2,4-trichlorobenzene at a former industrial contaminated site. Environmental Science & Technology, **39** (9), **2005**.

11. TORRES P., TRISTÃO DA CUNHA R., MICAELO C., RODRIGUES A.D.S. Bioaccumulation of metals and PCBs in Raja clavata. Science of the Total Environment, **573**, **2016**.

12. MONFERRAN M.V., ECHENIQUE J.R., WUNDERLIN D.A. Degradation of chlorobenzenes by a strain of Acidovorax avenae isolated from a polluted aquifer. Chemosphere, **61** (1), **2005**.

13. STUART-SMITH S.J., JEPSON P.D. Persistent threats need persistent counteraction: Responding to PCB pollution in marine mammals. Marine Policy, **84**, **2017**.

14. CZEGENY Z., JAKAB E., BLAZSO M., BHASKAR T., SAKATA Y. Thermal decomposition of polymer mixtures of PVC, PET and ABS containing brominated flame retardant: Formation of chlorinated and brominated organic compounds. Journal of Analytical and Applied Pyrolysis, **96**, **2012**.

15. FIELD J.A., SIERRA-ALVAREZ R. Microbial degradation of chlorinated benzenes. Biodegradation, **19** (4), **2008**.

16. GAO S., YANG J.Y., LIU M., YAN H.Z., LI W.X., ZHANG J.Q., LUO Y.B. Enhanced photovoltaic performance of CdS quantum dots sensitized highly oriented two-end-opened TiO_2 nanotubes array membrane. Journal of Power Sources, **250**, **2014**.

17. LI J., ZHAO L., WANG S.M., HU J.H., DONG B.H., LU H.B., WAN L., WANG P. Great improvement of photoelectric property from co-sensitization of TiO_2 electrodes with CdS quantum dots and dye N719 in dye-sensitized solar cells. Materials Research Bulletin, **48** (7), **2013**.

18. MENDEZ-MEDRANO M.G., KOWALSKA E., LEHOUX A., HERISSAN A., OHTANI B., RAU S., COLBEAU-JUSTIN C., RODRIGUEZ-LOPEZ J.L., REMITA H. Surface Modification of TiO_2 with Au Nanoclusters for Efficient Water Treatment and Hydrogen Generation under Visible Light. Journal of Physical Chemistry C, **120** (43), **2016**.

19. LU Y. Recent Progress in Crystal Facet Effect of TiO_2 Photocatalysts. Acta Physico-Chimica Sinica, **32** (9), **2016**.

20. WANG J., WANG X., LIU X.L., ZHU T.Y., GUO Y.Y., QI H. Catalytic oxidation of chlorinated benzenes over V_2O_5/TiO_2 catalysts: The effects of chlorine substituents. Catalysis Today, **241**, **2015**.

21. OBERG T., BERGBACK B., FILIPSSON M. Catalytic effects by metal oxides on the formation and degradation of chlorinated aromatic, compounds in fly ash. Chemosphere, **71** (6), **2008**.

22. LI C., JIANG F., SUN D., QIU B. Catalytic ozonation for advanced treatment of incineration leachate using (MnO_2-Co_3O_4)/AC as a catalyst. Chemical Engineering Journal, **325**, **2017**.

23. ZHANG D.E., REN L.Z., HAO X.Y., PAN B.B., WANG M.Y., MA J.J., LI F., LI S.A., TONG Z.W. Synthesis and photocatalytic property of multilayered Co_3O_4. Applied Surface Science, **355**, **2015**.

24. LIN S.J., SU G.J., ZHENG M.H., JIA M.K., QI C.S., LI W. The degradation of 1,2,4-trichlorobenzene using synthesized Co_3O_4 and the hypothesized mechanism. Journal of Hazardous Materials, **192** (3), **2011**.

25. GAO L.B., DIWU J.T., ZHANG Q., XU H.Y., CHOU X.J., TANG J., XUE C.Y. A Green and Facile Synthesis of Carbon-Incorporated Co3O4 Nanoparticles and Their Photocatalytic Activity for Hydrogen Evolution. Journal of Nanomaterials, **2015**.

26. XU H.Y., GAO L.B., ZHANG Q., LI J.Y., DIWU J.T., CHOU X.J., TANG J., XUE C.Y. Preparation Method of Co_3O_4 Nanoparticles Using Degreasing Cotton and Their Electrochemical Performances in Supercapacitors. Journal of Nanomaterials, (2), **2014**.

27. JANA T.K., PAL A., CHATTERJEE K. Magnetic and photocatalytic study of Co_3O_4-ZnO nanocomposite. Journal of Alloys and Compounds, **653**, **2015**.

28. ZHANG Y., HUANG J., DING Y. Porous Co_3O_4/CuO hollow polyhedral nanocages derived from metal-organic frameworks with heterojunctions as efficient photocatalytic water oxidation catalysts. Applied Catalysis B: Environmental, **198**, **2016**.

29. CHEN G., SI X., YU J., BAI H., ZHANG X. Doping nano-Co_3O_4 surface with bigger nanosized Ag and its photocatalytic properties for visible light photodegradation of organic dyes. Applied Surface Science, **330**, **2015**.

30. XIAO Q., ZHANG J., XIAO C., TAN X. Photocatalytic degradation of methylene blue over Co_3O_4/Bi_2WO_6 composite under visible light irradiation. Catalysis Communications, **9** (6), **2008**.

31. KIM T.Y., MIN B.J., KIM S.J., CHO S.Y. Photocatalytic Degradation of 2,4-Dinitrophenol Using TiO_2 in Aqueous Solution. Journal of Nanoscience and Nanotechnology, **10** (5), **2010**.

32. WU C.H. Photodegradation of CI Reactive Red 2 in UV/TiO_2-based systems: Effects of ultrasound irradiation. Journal of Hazardous Materials, **167** (1-3), **2009**.